JOURNAL OF GEOPHYSICAL RESEARCH, VOL. 85, NO. A13, PAGES 7613-7624, DECEMBER 30, 1980

PIONEER VENUS PLASMA OBSERVATIONS OF THE SOLAR WIND-VENUS INTERACTION

J. D. Mihalov and J. H. Wolfe

Space Science Division, NASA Ames Research Center, Moffett Field, California 94035

D. S. Intriligator

Physics Department, University of Southern California, Los Angeles, California 90007

Abstract. Collection of data from the Ames plasma analyzer on the Pioneer Venus orbiter has permitted long-term measurements of the interaction of the solar wind with Venus. This paper presents a mapping of the ionosheath flow field, as well as plasma measurements in the distant ionosheath and near the distant plasma cavity ($\sim$ 10 Venus radii downstream), a summary of observations of jumps in the solar wind proton parameters across Venus' bow shock, and also the apparent detection of ionospheric O^+ accelerated up to solar wind speeds downstream in Venus' ionosheath.

Introduction

Spacecraft observations of the interaction of the solar wind with Venus began with Mariner 2 in December 1962 and continued with Mariners 5 and 10 and Venera 4 and 6 [Russell, 1979] (see also Shefer et al. [1979]). Prior to the Pioneer Venus orbiter, extended studies beginning in October 1975 were possible with observations from the Venus satellites, Venera 9 and 10 [Vaisberg et al., 1976; Gringauz et al., 1976; Verigin et al., 1978; Smirnov et al., 1979]. In particular, results for the location and shape of Venus' bow shock, electron number density contours to 5 R_V (planet-centered Venus radii) in Venus' shadow, observation of an inner plasma boundary to the ionosheath downstream from Venus [Romanov et al., 1979], and some positive ion spectra that show features of the solar wind-Venus interaction were reported from Venera 9 and 10 data.

The Pioneer Venus orbiter spacecraft was launched on May 20, 1978. A summary of the Pioneer Venus orbiter mission is given by Colin [this issue]. In this paper, an intensive presentation of the plasma flow field in the terminator region of Venus' ionosheath is given, as well as a summary of jumps of plasma parameters across Venus' bow shock, and evidence for loss of ionospheric ions to Venus' ionosheath. Also, a record of solar wind speed variations following arrival of the orbiter at Venus on December 4, 1978, is presented.

Instrumentation

The Pioneer Venus orbiter plasma analyzer experiment uses 90° electrostatic deflection between quadrispherical analyzer plates. Then the plasma is detected by five separate current collectors, each at the input to an attendant electrometer amplifier. The mean radius of the deflection plates is 12 cm, and they are separated by 1 cm. The entrance aperture views normal to the spacecraft spin axis, which is approximately perpendicular to the ecliptic plane.

The deflection plate voltages of this experiment are programmed either to sample energy windows centered from 50 to 8000 V energy per unit charge (E/q) in 32 logarithmically spaced steps, or just the first 24 of these steps, both for positive ions. In addition, the instrument samples energy windows from 3 to 250 V E/q in 15 logarithmically spaced steps, for either positive ions or electrons. Except in special operating modes, the energy steps occur once every spacecraft revolution (about 12 s while in orbit around Venus), although there are electrometer stabilizations and detailed scan data interspersed. The experiment's memory capacity is sufficient to store one complete energy spectrum with its associated detailed scan data in order to minimize sample aliasing. More complete descriptions of this plasma experiment are given by Colin and Hunten [1977] and Intriligator et al. [1980] and further information on calibration and instrument response may be found in a description of the Pioneer 10 and 11 plasma experiments [McKibbin et al., 1977].

Except for some peak proton speeds (shown subsequently on Figure 1), the proton plasma parameters presented in this paper are obtained from the best least-squares fits of a convecting, isotropic temperature, Maxwellian proton velocity distribution, to proton electrometer currents measured in flight. Instrument angular and energy response characteristics are accounted for before the least-squares calculation is performed. Peak proton speeds, on the other hand, are obtained from the value of E/q at the spectral peak obtained from interpolated proton electrometer currents.

Summary of Interplanetary Conditions

Figure 1 extends the records published earlier [Wolfe et al., 1979; Intriligator et al., 1979] of variations of the solar wind speed since the Pioneer Venus orbiter arrived at Venus. The figure gives peak proton speeds in the free stream solar wind as near as possible to noon UT of each day. For some orbits with dayside periapses, when the aberration of the solar wind flow direction due to Venus' orbital motion, and variations of solar wind flow direction are neglected, one might expect that for average solar wind conditions there will be few plasma samples in the free stream solar wind [cf. Elphic et al., 1980]. We noticed some orbits with dayside periapses for which few realtime, free stream samples appeared present but still attempted to obtain these daily peak speed samples both outside of the ionosheath and away from the region just outside the bow

Paper number 80A0733.

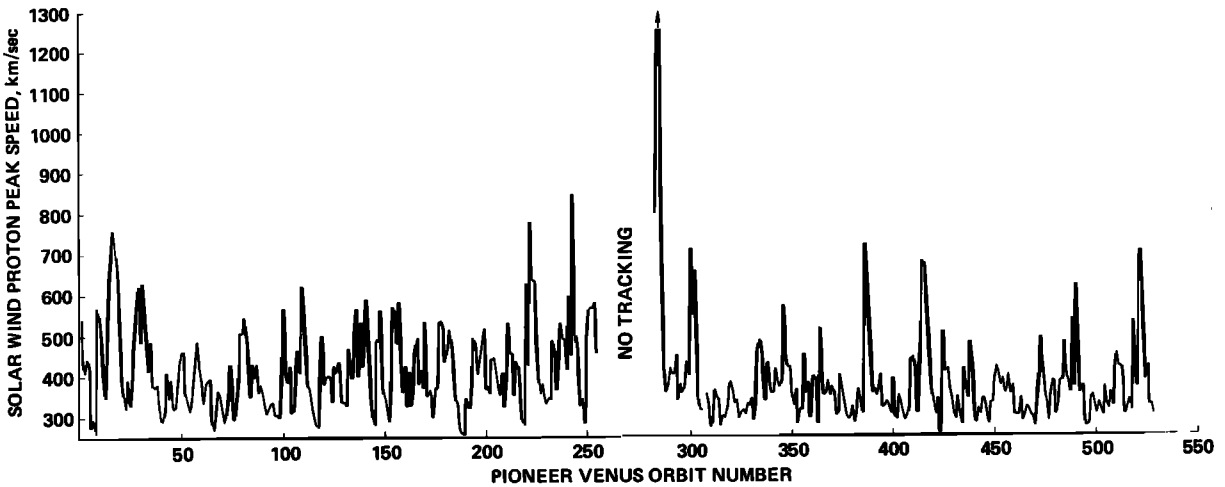

Fig. 1. Daily values of solar wind proton peak speed from the Ames plasma analyzer on the Pioneer Venus orbiter from injection into orbit to orbit 528.

shock where there might be significant upstream perturbations of the solar wind. The gap in the record from August 17 through September 11, 1979, (orbits 256 to 281) corresponds with times when Venus was near superior conjunction and the spacecraft was not tracked.

As noted previously [Intriligator et al., 1979], while some of the many high speed streams observed appear to be separated by the 28.0-day synodic rotation period of the sun, there are many additional streams for which this separation in time cannot be identified, so that there is no strong tendency for repetitive streams. The fact that this speed record exceeds 700 km s^{-1} only seven times (on December 20-21, 1978, on July 14, August 4, September 12-15, September 30, and December 26, 1979, and on May 10, 1980) indicates the relatively low frequency with which extreme cases for the solar wind interaction with Venus can be found in this period of the data. (These dates correspond to orbits 16-18, 222, 243, 282-5, 299, 386 and 522, respectively.) The five cases in 1979 of these high speeds probably correspond to large impulsive or solar flare events originating from the solar hemisphere opposite to the earth, rather than with quasi-stable high speed streams. Numerous interplanetary shocks have apparently passed Venus since this spacecraft was injected into orbit, but we have not yet enumerated these events. Some specific events of this type include those on December 11, 1978 (orbit 9) [Wolfe et al., 1979], on May 29, 1979 (orbit 175), observed in the ionosheath [Elphic et al., this issue] and mentioned later in this article, and one apparently observed in the ionosheath during orbit 219, also mentioned later. Finally, this speed record appears to have more frequent times with the peak speed below about 350 km s^{-1} after orbit 300, compared with the case from injection into orbit, up to orbit 300. This observation presumably is related to a decrease in solar activity.

Figure 2 shows daily estimates, obtained as near to noon UT as possible each day during 1979,

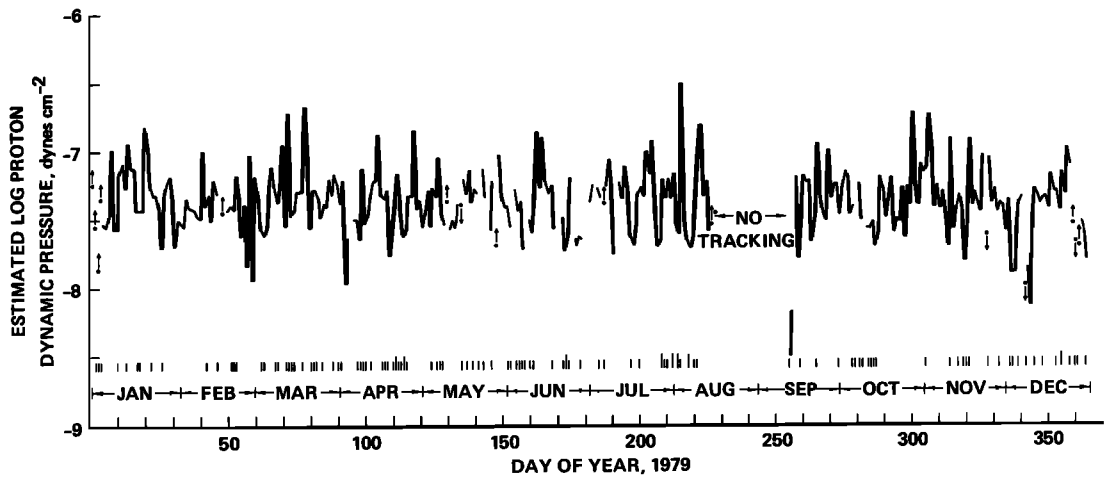

Fig. 2. Logarithms of daily estimates of proton dynamic pressure for 1979 from Pioneer Venus orbiter plasma data. The vertical lines at the bottom of the plot show where the proton velocity distributions appeared to have significant high-energy nonthermal components, with the longer vertical lines indicating particularly large nonthermal components (representing pressures $\gtrsim$ 30% of the plotted values).

of the free-stream solar wind proton dynamic pressure, nmv^2, at the orbiter. Here n is the measured proton number density, m is the proton mass, and v is the unaberrated proton bulk speed. Generally, the extreme values on this plot are not coincident with those of the peak speed plot of Figure 1. Sometimes the peak pressures appear in solar wind stream regions characteristic of compression (enhanced proton number density) that precede speed increases, and sometimes they apparently appear at noncompressive density enhancements [Feldman et al., 1978]. Since the peak values on the pressure plot are usually only one day wide, a fairly rapid variation with time of the pressure is indicated, and the peak amplitudes of these excursions should exceed the plotted values, which tend to be selected at a fixed time each day. The highest plotted point represents a pressure of 3.0×10^{-7} dyn cm^{-2} on August 4 (orbit 243). The lowest plotted estimate, at a pressure only 1/130 of the highest value (although a moderate nonthermal component should augment it), occurs only 39 days later (orbit 282).

Indications of high energy nonthermal proton velocity distributions, obtained from visual inspection of the least-squares fits and given by the vertical lines at the bottom of Figure 2 [Mihalov et al., 1979], show where the plotted pressure estimates are lower limits, owing to the non-Maxwellian character of the distribution functions at those times. Vertical lines longer than the others show where these nonthermal portions of the distribution functions are particularly large (representing pressures $\gtrsim$ 30% of the plotted values). No evidence has been found that these observations of nonthermal velocity distributions are due to a spurious effect, e.g., aliasing. Instances for which more than one Maxwellian proton distribution seemed simultaneously present in the solar wind were not selected for Figure 2.

Jumps in Plasma Parameters Across Venus' Bow Shock

The jumps of the solar wind parameters from the free stream values are observed in the plasma analyzer data each time the Pioneer Venus orbiter crosses Venus' bow shock into the ionosheath from the upstream flow, or vice versa. On Figure 3, the solar wind bulk speed jumps, v_D/v_U (D indicates downstream and U indicates upstream), and upper and lower limits, observed across Venus' bow shock, for 71 different orbits, from orbit 1 to orbit 243, are plotted against approximate values for the solar zenith angle (SZA). A reference curve is also given for the variation of the speed jumps for an axisymmetric gas dynamic shock analogy, for a sonic Mach number of 8, $\gamma = 5/3$, and a constant scale height ionopause shape with 0.1 R_V altitude at the stagnation point [Spreiter et al., 1970]. The difference in this case between the constant scale height and gravitationally varying scale height ionopause shapes and resulting flow fields is small [Spreiter and Stahara, this issue; Spreiter et al., 1970]. Although there is sizable scatter in the observed data, due probably to several causes, the points follow the trend of the reference curve. Part of this scatter is due to the range of Mach numbers associated with the data. However, for most of this range of Mach numbers, gas dynamic calculations show that for SZA > 50°, the variation of the velocity jump ratio with Mach number is only a few percent or less [Stahara et al., 1979] (also J. R. Spreiter, private communication, 1979). The one case on Figure 3 for which the ratio exceeds unity appears to be a time when the free stream speed was rising as the shock was crossed; such time variations are fairly frequent, and consequently somewhat difficult to eliminate in these data, and may contribute to the scatter. Finally, some MHD effects are not included in the gas dynamic model. The speed jumps of Figure 3 are not corrected for aberration, but an account of this effect is not expected to change the figure significantly. Study of the scatter in terms of the angle between the shock and the upstream magnetic field has not yet been possible. Data from the general time interval of Figure 3 were used to determine a shock surface model, and then these angles were determined first for subsequent times (C. T. Russell, private communication, 1980).

The jumps of solar wind proton number density across Venus' bow shock have been studied as a function of SZA, for 28 different orbits from orbit 1 to orbit 60 (36 shock crossings; SZA range 61° to 110°). There appears to be evidence at times for a density enhancement at the shock, similar to the one reported at the earth [Wolfe and McKibbin, 1968], so plasma parameters were calculated more frequently than the usual case to study the proton density jumps, when relatively more rapid time variations were present. Cases with many multiple shock crossings, sizable temporal variations, or ionosheath flow changes too rapid for accurate least-squares calculation of plasma parameters were eliminated also. (Owing to the configuration of the orbit, rapid changes of ionosheath density with position occasionally appear to be a significant source of uncertainty in the density determination). The density jump data were separated into three ranges of upstream sonic Mach number. Various values for solar wind electron temperature were assumed to calculate the sonic Mach numbers.

The density jump data appeared to scatter widely below the value of 4, and there were eight additional cases above 5.4. The gas dynamic analogy did not appear to be followed particularly closely, although changes in the parameters of that model, such as the Mach number and γ, would permit some variation of the model values. Inclusion of the magnetic field terms in the momentum and energy conservation equations [cf. Spreiter and Stahara, this issue; Spreiter et al., 1966] would permit the density jump to drop well below the value of 4, for whistler mode shocks, with Mach numbers less than 5 [Tidman and Krall, 1971] (see also Spreiter and Rizzi [1974]). Out of the three ranges of sonic Mach number, the low Mach number cases ($M < \sim 4.5$) tended to be associated with the lowest density jumps (7 cases; average density jump $\sim$ 1.9). The nigh Mach number cases ($M > \sim 6$) seemed to cluster with the cases from the remaining, intermediate Mach number range of the three ranges, with proton density jumps closer to gas dynamic model values of between 3 and 4. The eight cases with density jump values exceeding 5.4 had an average Mach number of $\sim$ 5.2 and are the

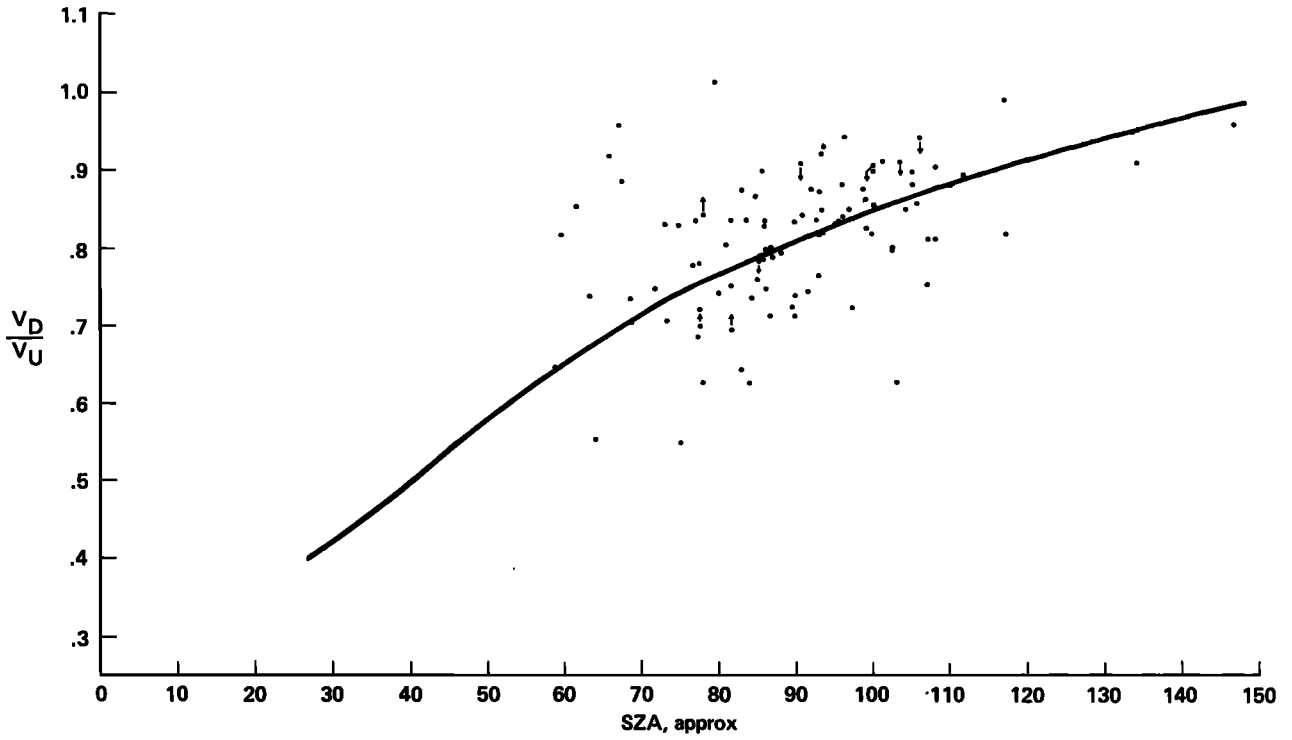

Fig. 3. Estimated solar wind proton bulk speed jumps, and upper and lower limits, observed across Venus' bow shock for 71 different orbits, plotted against approximate values for solar zenith angle in degrees. A calculated curve from a gas dynamic analogy is also given.

evidence for a density enhancement referred to above at the shock. It is unknown why this phenomenon is only observed occasionally. At Venus it is not easy to assign post-shock number densities for jump determinations when this density enhancement is present, if it must be excluded for these determinations, as it appears to be relatively wide in comparison with the ionosheath thickness, so that a shock model with such a feature seems required. Furthermore, it is not easy to clearly separate protons from helium in the ionosheath data, but this effect is not likely to introduce a large density error and may be studied by making various assumptions for the helium velocity distributions. In addition, it may be that sometimes there are relatively large fluctuations with time in the ionosheath proton velocity distribution, which could cause our calculation of temperature to be erroneously somewhat high, and the calculated density to be somewhat low; this possibility may be studied further, but is not expected to be particularly frequent.

The average and median temperature jumps, for 5° increments of SZA, observed across Venus' bow shock during 69 orbits from orbit 1 to orbit 243 are given on Figure 4. The average and median values lie below the line, also given on the figure, that represents the calculated temperature jump for the same gas dynamic model as used for Figure 3 (upstream sonic Mach number, M, of 8; γ = 5/3). The calculated temperature jumps arise from use of the perfect gas law, p = knT, with p the thermodynamic pressure, n the number density, and T the temperature; k is Boltzmann's constant; these jumps are given by $(T_D/T_U) = 1 + 1/2\ (\gamma - 1)\ M^2\ (1-(v_D/v_U)^2)$ [Spreiter et al., 1966]. For a fully ionized hydrogen plasma, it is reasonable to consider T as the sum of the electron and ion temperatures, so that the calculated temperature jumps are for this sum. We observe that the measured temperature jumps of the protons tend to be just above half of the calculated values. Separate temperature jumps for protons and electrons may be derived, one from another, by using the Alfvèn Mach number, the upstream plasma β , the flow deflection, and the angle between the shock normal and the upstream magnetic field vector [Sanderson and Uhrig, 1978].

Following the discussion of Chao and Goldstein [1972] about the energy and momentum flux of plasma waves and of Tidman and Krall [1971] about turbulent shocks, Venus' shock jumps may be modified owing to the enhanced electrostatic (electron plasma oscillations) and whistler mode plasma waves observed there [Scarf et al., this issue], in comparison with the case at earth. Finally, we mention one example of quite high ion heating observed at Venus' bow shock, in which a proton temperature jump of a factor of 17 was measured. (For this case, the upstream sonic Mach number was estimated to be 8.)

Flow Field and Ionospheric Ions in Venus' Ionosheath

The Ames plasma analyzer provides excellent capability for vector plasma velocity measurements, so that detailed study of the deflection of

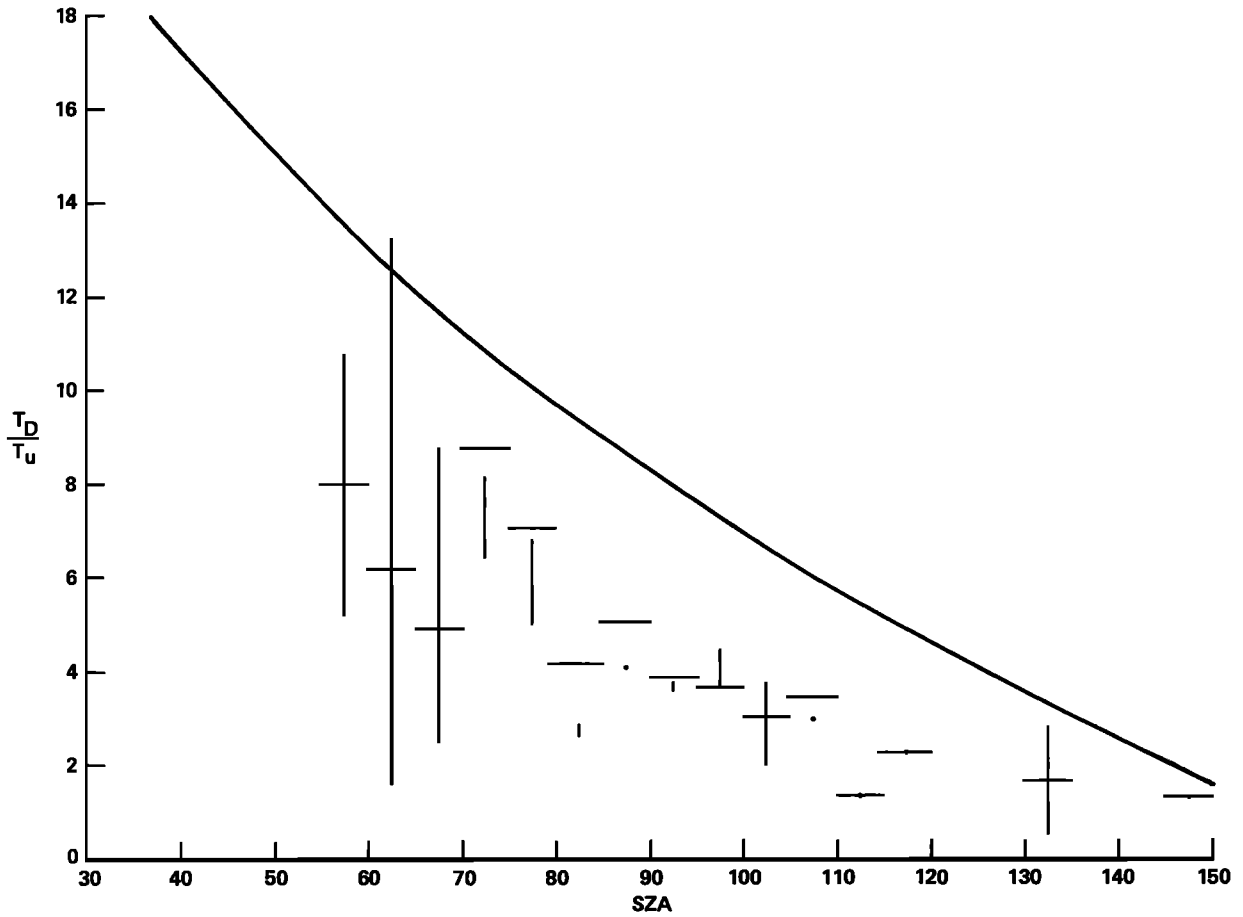

Fig. 4. Average (horizontal lines) and median (points and vertical lines) values for solar wind proton isotropic temperature jumps, observed across Venus' bow shock for 69 different orbits, plotted as in Figure 3 but for 5° increments of SZA.

the solar wind in Venus' ionosheath is possible. Figure 5 gives a portion of the plasma proton flow field observed around Venus in the ionosheath from this experiment. The proton data were used to obtain bulk speeds and vector flow directions, using the least-squares procedure described above. The vector velocities of the orbiter spacecraft, and of Venus itself, have both been subtracted; consequently, the flow field is presented as if Venus and the spacecraft were both stationary in the solar wind. For each observation, the plane of the figure is the sun-Venus-orbiter plane, and the projections of the individual flow vectors onto that plane are plotted. The locations of the observations are at the tails of the vectors. Data from 109 orbits were used, ranging from orbit 1 to orbit 191. Note that the flow directions on Figure 5 have not been corrected for small tips of the spacecraft spin axis, of order 1° or less. Correction for deviations of the upstream solar wind flow directions has not been done for this figure. Such corrections could only be attempted, using measurements from only a single spacecraft, by interpolation between values observed before the spacecraft passes behind the bow snock, and free stream values observed after the ionosheath passage, after the bow shock is again crossed. Since the flow directions in the free stream frequently show large fluctuations in time periods comparable to those of ionosheath traversals (as indicated by sample cases presented by Spreiter and Stahara [this issue]), the correction procedure just described would usually not be particularly reliable.

On the bottom portion of Figure 5 a sample streamline is also given and ionopause and shock shapes indicated by solid lines. These boundaries are taken from a single-fluid, continuum model for solar wind flow (gas dynamic Mach number, M, of 8, ratio of specific heats $\gamma = 5/3$) past a nonmagnetic planet with an ionosphere with a gravitationally varying scale height, and 0.1 R_V ionopause altitude at the stagnation point [Spreiter and Stahara, this issue]. The projected bulk flow directions appear to agree fairly well, in a mean sense, with the streamline, except possibly near the shock. It should be noted that the plotted flow direction projections are for a large range of Mach numbers, without selection. Some measure of the upstream flow speed is available from the magnitudes of the plotted vectors. The plotted flow field appears completely consistent with deflection around a blunt obstacle, together with the upstream standing bow shock that has been discussed by Slavin et al. [1979a,b, this issue] and Russell et al. [1979b]. The data clearly show that conditions occur with ionosheath flow both at lower altitudes than the plotted ionopause, and outside of the plotted shock location. Both features can be readily accounted for in terms of

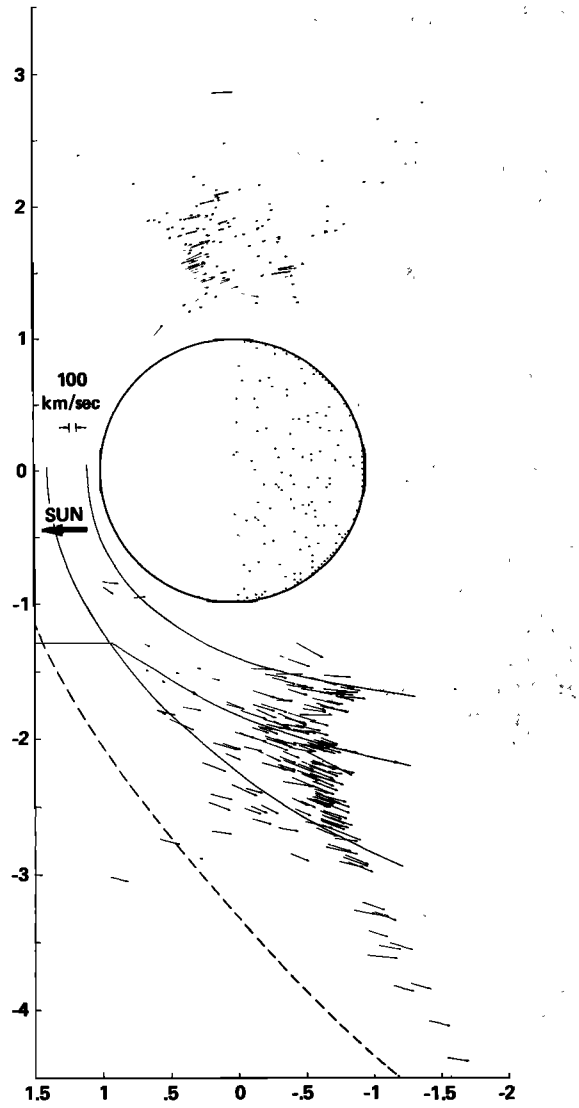

Fig. 5. Ionosheath flow field around Venus as measured by the Ames plasma analyzer and presented in a common plane. Each flow vector is projected onto its unique sun-Venus-orbiter plane. Vectors measured north of Venus' orbital plane are plotted in the upper half of the figure, while the remaining vectors were measured south of Venus' orbital plane. A gas dynamic flow streamline is shown that is appropriate to a sonic Mach number M of 8 and a particular ionopause shape. The corresponding bow shock and a bow shock for M = 2 (dashes) are also shown.

variations of ionosphere and free stream solar wind conditions. A dashed line on Figure 5 gives a gas dynamic bow shock location for M = 2 [Stahara et al., 1979] (same ionopause as shown, except that a constant scale height is assumed for the ionosphere), and shows that the more distant ionosheath measurements are consistent with lower Mach numbers. The upstream sonic Mach numbers we calculate for the two orbits with the most distant ionosheath samples plotted on the bottom half of Figure 5, however, are not among the lowest such values, being between 6 and 7. This discrepancy may be due to variation of the ionopause shape, or MHD effects. A more complete comparison of Pioneer Venus ionosheath observations with gas dynamic calculations is being prepared (see also Spreiter and Stahara [this issue]).

A mantle region, in which electron spectra gradually change from ionospheric characteristics to those of the ionosheath, has been identified from retarding potential analyzer data [Spenner et al., this issue]. The orbiter plasma analyzer observations during time periods for which retarding potential analyzer and mantle data have been presented [Spenner et al., this issue] are as follows. For orbit 66, intense ionosheath plasma fluxes are observed well into the inbound mantle region. However, these fluxes appear to begin to drop at ∿ 1952:45 UT, February 8, 1979, and seem to be below the experiment's unoptimized maximum flux scan threshold by ∿ 1955:00 UT, about one-third of the duration of the passage through the mantle. Polar scan data [cf. Intriligator et al., 1980] taken about two-thirds through, however, show peak plasma fluxes (200 - 300 V E/q) moving southward into the cavity; such observations are discussed later. For the outbound passage, only sporadic fluxes suggestive of ionospheric ions incident from the spacecraft ram velocity direction, but with intensities weaker than the case published earlier [Wolfe et al., 1979], are observed in the mantle. Ionosheath fluxes only begin to be observed at ∿ 2030:15 UT outside the mantle, and were not present at ∿ 2027:30 UT, about at the 'inner ionosheath boundary' as determined by Spenner et al. [this issue].

For orbit 168, ionosheath plasma is last observed at ∿ 2056:00 UT, May 21, 1979, outside the mantle, and is definitely absent by ∿ 2059:00 UT, about half through the mantle. In the inbound and outbound mantles, the ionosphere, and even during the first measurements in the outbound ionosheath, fairly continuous, weak plasma fluxes are apparently observed from the general direction along the spacecraft ram velocity. Ionosheath fluxes return within the outbound 'mantle,' at ∿ 2109:30 UT (after this observation of ionosheath fluxes, experiment energy returned to the low end of its range which permitted the further brief apparent observation in the ionosheath of ions from the ram direction).

In the case of orbit 195, the ionosheath plasma disappears at ∿ 2145:30 UT, June 17, 1979, about at the retarding potential analyzer 'inner ionosheath boundary,' and only very weak plasma fluxes from the ram direction, or experiment background noise, are observed in the 'mantle.' To summarize this limited comparison of the two sets of data, the solar wind plasma experiment results are in agreement with the conclusion of Spenner et al. [this issue] that ionosheath plasma is not consistently excluded from their 'mantle.'

A few of the flow projections on Figure 5, among those that indicate the general tendency for the plasma to flow around the planet, suggest deflection into a cavity region. It is possible, but not likely, that the most extreme of these flow deflections, toward the cavity, are due to variations of the free-stream flow direction, rather than demonstrating a more general property of the flow. The relatively numerous flow deflections toward Venus' cavity reported by Intriligator et al. [1979], in comparison, some-

times arise from data samples too brief to obtain flow directions from least-squares fitting, the technique used to produce Figure 5. In addition, the flow vectors on Figure 5 are a different projection from those given in the earlier work. The axisymmetric projection used here permits more accurate portrayal of the magnitude of flow deflections toward the cavity, but the use of the complete least-squares results restricts the number of cases presented to a higher flux set in which large deflections may be less frequent. Finally, the two cases upstream of Venus that suggest flow into the planet, instead of deflections, actually correspond to deflection out of the plane of the figure, such that an extension of the flow vector does not intersect Venus, or probably even the ionopause.

The absence of vectors near the antisunward hemisphere of Venus in Figure 5 is due to low plasma densities there. Data from 16 orbits from orbit 59 to 95, for which the orbiter periapsis was on Venus' nightside, frequently showed the density of the streaming ionosheath plasma dropping below the normal experiment threshold well before the optical shadow of Venus was reached. Also, the low periapsis altitude, below the ionopause, accounts for a general lack of vectors on the dayside. Our observation of greatly diminished plasma fluxes in the optical shadow near Venus is in agreement with Venera 9 and 10 ion observations [Vaisberg et al., 1976; Gringauz et al., 1976; Verigin et al., 1978]. Venera 10 ion measurements also showed times when the 50 to 500 eV flux was unmeasurably low in Venus' optical shadow [Romanov et al., 1979]. There were some instances in the Pioneer observations (e.g., orbit 66 inbound) where extremely weak plasma fluxes in Venus' optical shadow were observed, with apparent flow directions toward Venus' orbital plane, also in agreement with one case reported from Venera 10 [Vaisberg et al., 1976]. In the more usual cases, ionosheath plasma was not observed beginning with altitudes well above the ionopause as located by L. H. Brace (private communication, 1979). However, for those usual cases, plasma was not observed within Venus' optical shadow either. Nevertheless, for a few of those usual cases, the uncertainties of the locations at which the plasma fluxes dropped below instrument threshold are large enough to include some locations within the optical shadow.

Figure 6 gives a projection onto Venus' orbital plane of the flow-field in Venus' ionosheath. Since flow directions over the poles seemed well behaved, an exhaustive analysis seemed unwarranted, and only a few (77) orbits of data were used, ranging from orbit 1 to orbit 211. The observations made both north and south of the planet are projected onto the same plane, without distinction. The flow field corresponds to unaberrated flow, as in the previous figure. The projections of the locations of the measurements are at the tails of the vectors, which are all drawn the same length. No unexpected results appear in this projection of the ionosheath flow field, which shows little deviation from the free stream condition, the expected situation for these measurements mostly above (or below) Venus' polar regions. Deviations of the upstream solar wind flow directions from the direction radially outward from the sun are probably the source of

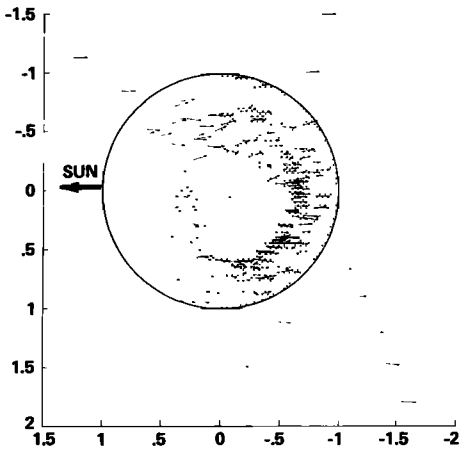

Fig. 6. Projection of Venus' ionosheath flow field onto the plane of Venus' orbit. All flow vectors are plotted with the same length.

some of the deviations of the flow projections from the antisolar direction.

Figure 7 shows plasma parameters (the aberrated proton speed, number density, isotropic temperature, and polar flow direction) from the inbound leg of orbit 176, for most of which the orbiter remained within Venus' ionosheath, as an example of data acquired from this region. Elphic et al. [this issue] present magnetic field magnitudes for this time period measured by the Pioneer Venus magnetometer. Positive polar flow angles correspond to southward flow. Discontinuous changes of these parameters at ∿0850, ∿1625 and ∿1955 UT are suggestive of bow shock crossings (an outbound crossing at the first time and inbound crossings for the two later times), although at these times the spacecraft location is not near the mean bow shock location obtained by Slavin et al. [1979a] (cf. Figure 1 of Elphic et al. [this issue]). Presumably, this mean bow shock location is for quasi-perpendicular shocks [Slavin et al., 1979]. (Apparently, a discontinuity also occurs at ∿1350 UT.) The spacecraft location during these times does not appear to be near enough to Venus' plasma cavity to identify clearly the decreased speed, and the regions of compression and rarefaction in plasma density measurements, observed there by other plasma experiments [Shefer et al., 1979; Vaisberg et al., 1976] (see also review article by Russell [1979]). The pronounced southward flow in the ionosheath during much of the time of Figure 7 is unusual. We have observed relatively large flow deflections associated with interplanetary shock events, so that this case is probably due to plasma flow characteristics that follow an interplanetary shock [cf. Elphic et al., this issue], and the distant ionosheath is probably disturbed. (Large disturbances of this sort were also apparently observed during orbits 219 and 220.)

On Figure 8, plasma parameters from the inbound leg of orbit 189 are shown. The distance scales at the top of the figure indicate a closer approach to Venus' optical shadow than for the case of orbit 176, and the approach is from the side toward which solar wind aberration would shift downstream plasma perturbations. A decrease

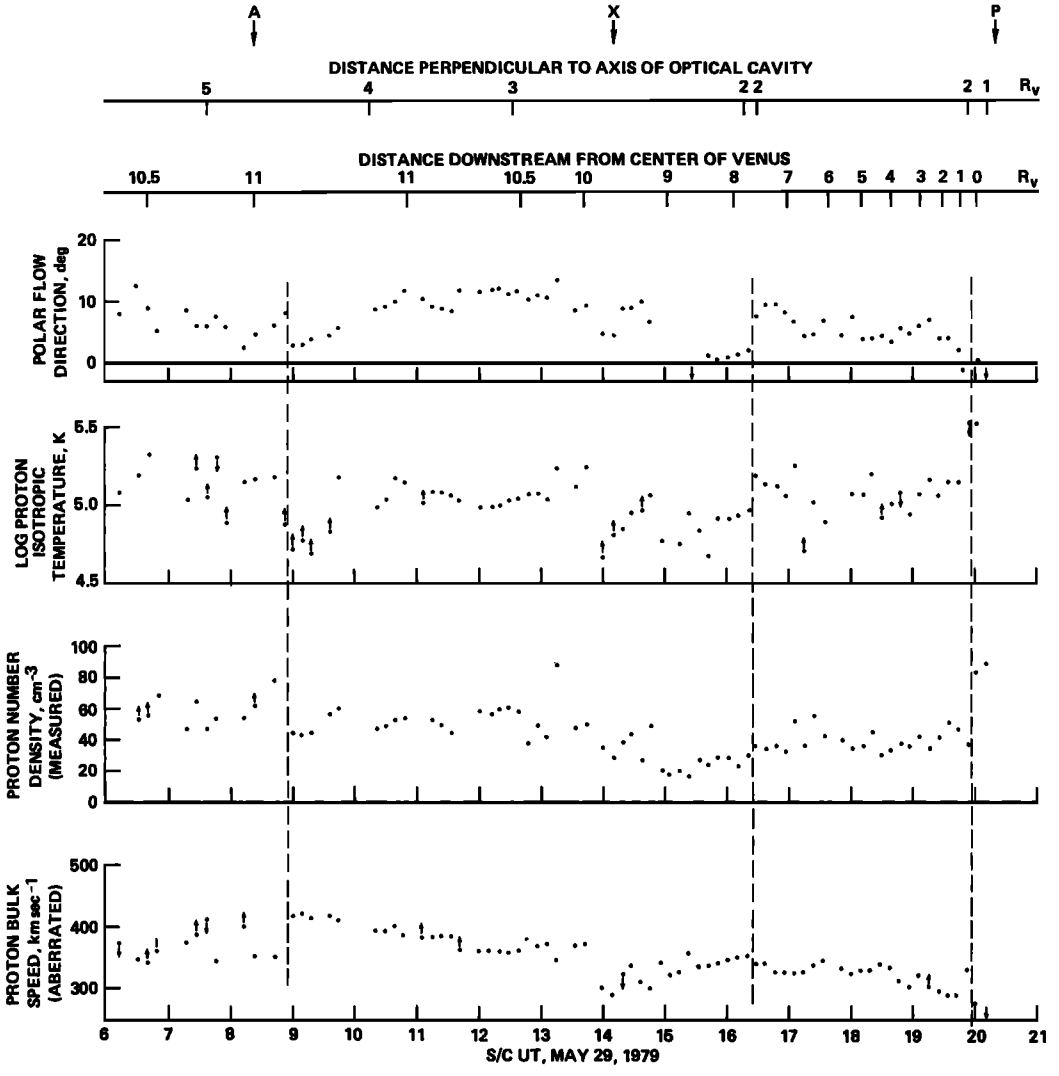

Fig. 7. Proton bulk speeds (aberrated), number densities, isotropic temperatures, and polar flow directions from the inbound leg of orbit 176. In some cases, upper or lower limits to these parameters are indicated with arrows. The times of orbiter apoapsis and periapsis are indicated by 'A' and 'P,' respectively. The time when the orbiter crosses Venus' orbital plane, moving northward, is indicated by 'X.' Distance scales at the top of the figure give spacecraft locations in Venus radii (R_V). Plasma parameter jumps suggestive of bow shock crossings are indicated by dashed lines.

of proton bulk speed is evident near the closest approach to the optical shadow, even as far as $\sim$ 10 R_V downstream from Venus. The proton temperature plot indicates some heating associated with the decreased speeds, which had been reported at locations closer to Venus [Romanov et al., 1979; Shefer et al., 1979; Vaisberg et al., 1976]. The horizontal bar from $\sim$1505 to $\sim$1645 UT on the speed plot shows when the plasma fluxes were below the sensitivity (unoptimized) of the plasma analyzer. Orbit 189 is the first one following the eight (orbits 181 to 188) for which the orbiter entered Venus' optical shadow near apoapsis [Colin, this issue]. Orbits 181, 186 and 188 have times similar to those in orbit 189 when plasma fluxes were not detected, as do some of the orbits following 189 (partly as a result of the aberration due to Venus' orbital motion). For orbits 182 to 185 and 187, part of the time the measurements were limited to 250 V E/q, or the experiment was turned off to conserve spacecraft battery power. The plasma analyzer also was turned off for the same reason when these distant occultations of the sun by Venus again occurred during orbits 406 to 412, in January 1980.

Plasma compression and rarefaction are not clearly shown in the proton number density plot for orbit 189, although those effects have been reported from earlier ion measurements closer to Venus [Bridge et al., 1967; Shefer et al., 1979]. (Compression is associated with the bow shock that has been discussed above; rarefaction is demonstrated better on orbit 186 during which the proton number density drops below 2 cm^{-3} in the cavity region, and is $\sim$ 10 cm^{-3} prior to entering the cavity.) The two horizontal bars from $\sim$1210 to $\sim$1500 UT, above the speed plot, indicate times when fluxes of ionospheric ions

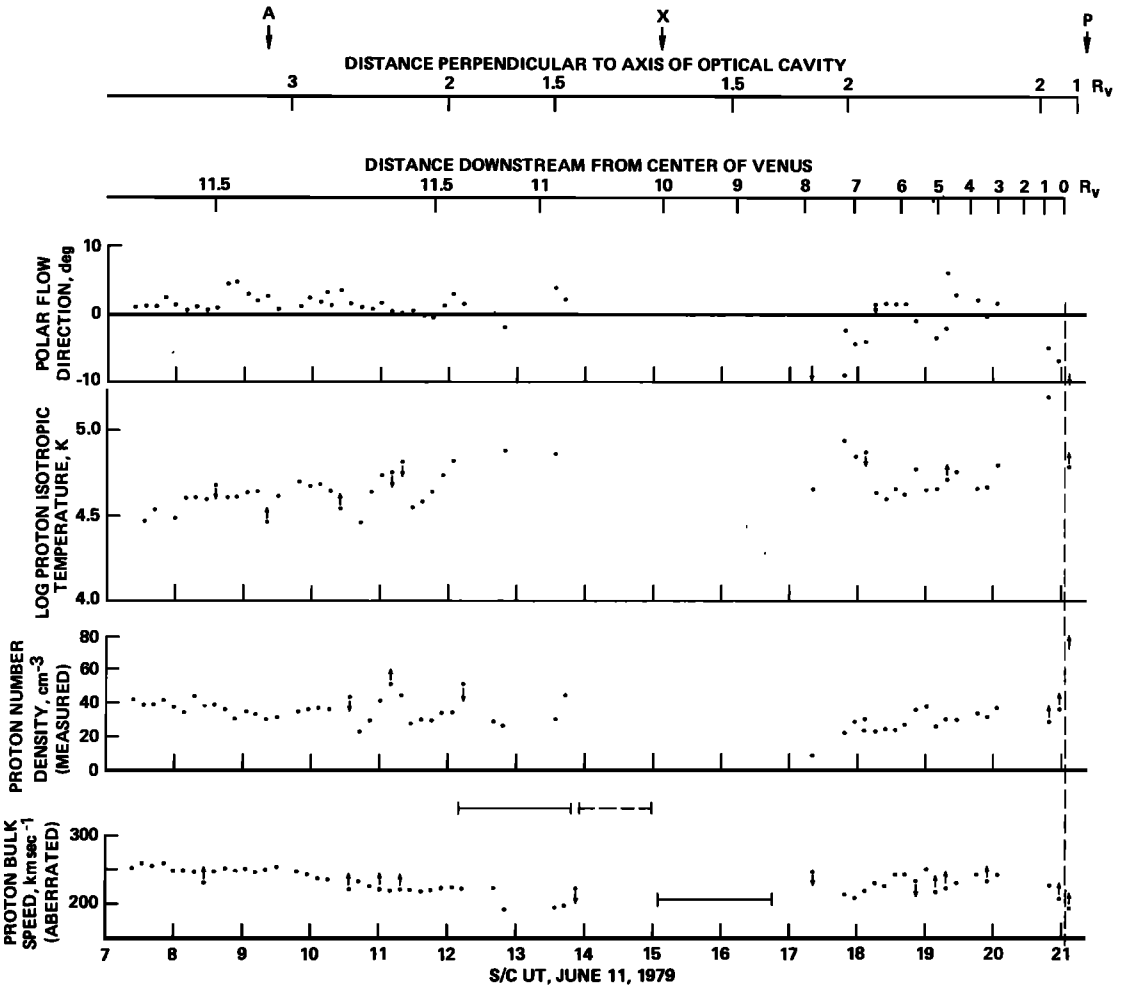

Fig. 8. Same as Figure 7 for the inbound leg of orbit 189. Three horizontal bars on the plot of proton bulk speeds show times when fluxes of ionospheric ions accelerated to ionosheath speeds are apparently observed or (∿1505 to ∿1645 UT) when plasma fluxes decreased below the experiment threshold.

(E/q >> E/q for protons), apparently accelerated to speeds characteristic of the ionosheath plasma, are observed. During the time interval of the first, solid horizontal bar, these ion fluxes are generally observed at $\gtrsim$ 4 keV E/q; during the second time interval, indicated with a dashed horizontal bar, these heavy ion fluxes are observed at decreasing E/q, generally below 3 keV. The decrease of E/q during the second time interval seems analogous to the general decrease of proton speed near the optical shadow that was discussed above.

Figure 9 is an example of such data. A non-modeled estimate of the proton velocity distribution function, obtained ignoring overlap of adjacent energy passbands of the experiment, is plotted against E/q. On this plot, ionosheath protons and helium together produce the left-hand peak. Our best values for the proton parameters at this time are indicated on Figure 8. It was not possible to readily distinguish helium from protons for the data of the left-hand peak of Figure 9, because of the apparent increased ionosheath proton temperatures near the cavity region, and the probability that the helium density is low at this time. Consequently, that peak was plotted as if all the measured currents were due to protons. The right-hand peak is consistent with an energy per unit charge appropriate to O^+ traveling at the bulk speed of the solar wind ions (E/q (high)/E/q (low) ∿ 4750 V/290 V = 16). The dashed line indicates the corresponding calculated experiment response to an O^+ distribution of 240 km s^{-1} aberrated bulk speed, with a ∿ 10^{-1} cm^{-3} number density and a ∿300,000 K isotropic temperature. The same secondary electron coefficient as for protons of the same E/q has been assumed. The location of this observation is 1.8 R_V perpendicular to the extended sun-Venus line and 11.3 R_V downstream from the center of Venus, as indicated also on Figure 8. The scavenged ions in this case have traveled some distance downstream in the ionosheath. Beginning about 40 minutes after this observation, lower energy particles appear simultaneously at two values of E/q for about an hour. The higher of the two values of E/q is similar to that for the Figure 9 protons, and the lower value is about 2/3 that of the higher. These observations are relatively close to Venus' optical shadow, and, in fact, about two and one-half hours after the case of Figure 9, the ionosheath ion

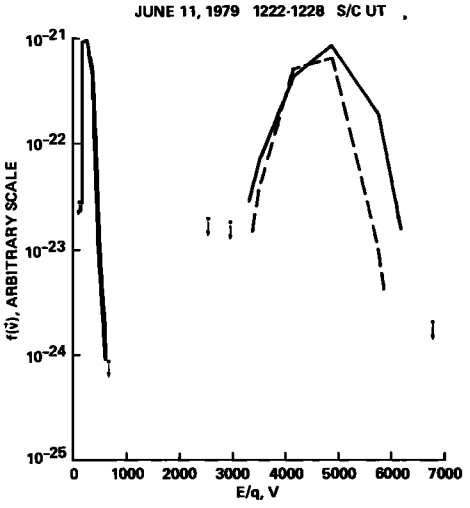

Fig. 9. Estimate of positive ion velocity distribution function, plotted with E/q as the abscissa, observed 11 radii downstream from Venus, in the ionosheath. The ionosheath protons and helium form the left-hand peak, while the right-hand peak probably arises from O^+ swept up from Venus' ionosphere. The dashed line is a fit of a convecting, isotropic temperature Maxwellian distribution to flight data for the right-hand peak.

fluxes dropped below the nominal sensitivity threshold of the plasma analyzer for about one hour and 40 minutes, as mentioned previously, and indicated on Figure 8. The low fluxes would be characteristic of measurements in the optical shadow itself, although that region was only approached from the direction in which normal solar wind aberration due to Venus' orbital motion would shift the planet's 'shadow' in the solar wind, and not entered, as also described above.

Apparent observations of heavy ions swept up into the ionosheath from Venus' ionosphere occur also forward of the location far downstream on the flanks of the cavity where the data of Figure 9 were acquired. The ion number density of the peak at higher E/q in the figure is estimated to be $\sim$ 1% of the ionosheath proton density.

The possibility for the addition of atmospheric atoms to the solar wind flow at Venus, usually through the mechanism of photoionization of neutrals, has been recognized for many years [Cloutier et al., 1969; Michel, 1971a,b; Hartle and Wu, 1973; Wallis, 1973; Cloutier et al., 1974; Pérez de Tejada and Dryer 1976; Bauer et al., 1977]. Detailed calculations of the trajectories of the photoions indicate that their energy distribution will be broad, with relatively broad, energy dependent angular distributions that are not aligned with the flow [Cloutier et al., 1974]. The dynamic characteristic of the size of Venus' ionosphere revealed by the initial Pioneer Venus observations [Knudsen et al., 1979; Brace et al., 1979], which were made during times of relatively high solar activity, leads to consideration of an alternative, impulsive mechanism for ion pickup by the solar wind [Brace et al., this issue].

We have examined the relative flow directions of the ionosheath protons and the apparent ionospheric ions for the 11 cycles of the experiment during the time period from $\sim$ 1210 to $\sim$ 1350 UT on Figure 8 when the more energetic component is generally observed at $\gtrsim$ 4 keV E/q. We found that generally the flow directions of the two components are about the same. However, near the middle of this interval only, when the proton density becomes particularly low, there is some evidence for deflection of the protons away from the direction of the more energetic component, by $\sim$ 10°, and toward the 'cavity' region. A similar deflection, but immediately behind Venus, was reported by Vaisberg et al. [1976], except that the relative energy of the more deflected component was not clearly identified in that publication. We do find a tendency for the angular distribution of the more energetic component to be much narrower than that of the ionosheath protons. This may suggest than an impulsive model for ion pickup [Brace et al., this issue] is favored over the photoionization mechanism, by these particular observations.

The identification of the scavenged ion as O^+ is consistent with the identification of this ion as most abundant near the outer fringes of Venus' dayside ionosphere [Taylor et al., 1979a,b,c, this issue; Bauer et al., 1979], where one expects the source of ionosheath heavy ions from simple considerations.

Summary

Interplanetary conditions for the 16 months following orbital injection of the Pioneer Venus orbiter have been summarized by records of daily samples of solar wind peak speeds and daily estimates of proton dynamic pressures. The record of peak speeds includes some extreme values, as in mid-September 1979 when four consecutive daily values were at or above 800 km s^{-1}. However, the largest modifications to Venus' ionosphere (and ionosheath) due to solar wind activity may be expected instead when the upstream pressure, rather than the upstream speed, takes extreme values [cf. Brace et al., this issue]. The days of the peak pressures generally are not coincident with those of maximum peak speed.

The solar wind flow directions are observed to be deflected around Venus in the ionosheath, as expected for an obstacle in supersonic fluid flow, with a standing upstream bow shock. Plots of the ionosheath flow field are consistent with published bow shock locations [Russell et al., 1979a; Slavin et al., 1979a], except for extreme examples. These plots are also consistent with no steadystate absorption of solar wind protons by Venus' dayside ionosphere, although a modest absorption ($\sim$ 10%) cannot be ruled out. Values for jumps of the proton speed, number density, and temperature across the bow shock itself scatter fairly widely. Scatter is expected due to variations of free-stream conditions (e.g., the Mach number) and of the ionopause (obstacle) shape. At low values of Mach number, MHD effects will introduce further scatter.

We found evidence for a density enhancement at Venus' bow shock at times, similar to that reported for the Pioneer 6 traversal of earth's bow shock [Wolfe and McKibbin, 1968]. The density jumps would tend to scatter even more than otherwise with such a feature present.

Flow toward a plasma cavity downstream from

Venus may be observed sporadically, as was reported earlier [Intriligator et al., 1979]. The most prominent signature of the cavity far downstream ($\sim$ 10 R_V) in the plasma analyzer data is a decrease in the proton flux. Also, the proton bulk speed decreases as the cavity is approached.

Finally, observation of ions much more energetic than protons suggests the sweeping up of ionospheric O^+ and its acceleration to ionosheath speeds.

Acknowledgments. We acknowledge J. R. Cowley for supplying approximate values for SZA and A. Barnes, R. C. Elphic, R. C. Whitten, and Prof. J. R. Spreiter for valuable discussions.

References

Bauer, S. J., L. H. Brace, D. M. Hunten, D. S. Intriligator, W. C. Knudsen, A. F. Nagy, C. T. Russell, F. L. Scarf, and J. H. Wolfe, The Venus ionosphere and solar wind interaction, Space Sci. Rev., 20, 413-430, 1977.

Bauer, S. J., T. M. Donahue, R. E. Hartle, and H. A. Taylor, Jr., Venus ionosphere: Photochemical and thermal diffusion control of ion composition, Science, 205, 109-112, 1979.

Brace, L. H., R. F. Theis, J. P. Krehbiel, A. F. Nagy, T. M. Donahue, M. B. McElroy, and A. Pedersen, Electron temperatures and densities in the Venus ionosphere: Pioneer Venus orbiter electron temperature probe results, Science, 203, 763-765, 1979.

Brace, L. H., R. F. Theis, W. R. Hoegy, J. H. Wolfe, J. D. Mihalov, C. T. Russell, R. C. Elphic, and A. F. Nagy, The dynamic behavior of the Venus ionosphere in response to solar wind interactions, J. Geophys. Res., this issue.

Bridge, H. S., A. J. Lazarus, C. W. Synder, E. J. Smith, L. Davis, Jr., P. J. Coleman, Jr., and D. E. Jones, Mariner V: Plasma and magnetic fields observed near Venus, Science, 158, 1669-1673, 1967.

Chao, J. K., and B. Goldstein, Modification of the Rankine-Hugoniot relations for shocks in space, J. Geophys. Res., 77, 5455-5466, 1972.

Cloutier, P. A., M. B. McElroy, and F. C. Michel, Modification of the Martian ionosphere by the solar wind, J. Geophys. Res., 74, 6215-6228, 1969.

Cloutier, P. A., R. E. Daniell, Jr., and D. M. Butler, Atmospheric ion wakes of Venus and Mars in the solar wind, Planet. Space Sci., 22, 967-990, 1974.

Colin, L., The Pioneer Venus program, J. Geophys. Res., this issue.

Colin, L., and D. M. Hunten, Pioneer Venus experiment descriptions, Space Sci. Rev., 20, 451-525, 1977.

Elphic, R. C., C. T. Russell, J. A. Slavin, and L. H. Brace, Observations of the dayside ionopause and ionosphere of Venus, J. Geophys. Res., this issue.

Feldman, W. C., J. R. Asbridge, S. J. Bame, and J. T. Gosling, Long-term variations of selected solar wind properties: Imp 6, 7, and 8 results, J. Geophys. Res., 83, 2177-2189, 1978.

Gringauz, K. I., V. V. Bezrukikh, T. K. Breus, T. Gombosi, A. P. Remizov, M. I. Verigin, and G. I. Volkov, Plasma observations near Venus onboard the Venera 9 and 10 satellites by means of wide-angle plasma detectors, in Physics of Solar Planetary Environments, vol. 2, edited by D. J. Williams, pp. 918-932, American Geophysical Union, Washington, D. C., 1976.

Hartle, R. E., and C. S. Wu, Effects of electrostatic instabilities on planetary and interstellar ions in the solar wind, J. Geophys. Res., 78, 5802-5807, 1973.

Intriligator, D. S., H. R. Collard, J. D. Mihalov, R. C. Whitten, and J. H. Wolfe, Electron observations and ion flows from the Pioneer Venus orbiter plasma analyzer experiment, Science, 205, 116-119, 1979.

Intriligator, D. S., J. H. Wolfe, and J. D. Mihalov, The Pioneer Venus orbiter plasma analyzer experiment, IEEE Trans. Geosci. Remote Sensing, GE-18, 39-43, 1980.

Knudsen, W. C., K. Spenner, R. C. Whitten, J. R. Spreiter, K. L. Miller, and V. Novak, Thermal structure and major ion composition of the Venus ionosphere: First RPA results from Venus orbiter, Science, 203, 757-763, 1979.

McKibbin, D. D., J. H. Wolfe, H. R. Collard, H. F. Savage, and R. Molari, Plasma analyzer for the Pioneer Jupiter mission, Space Sci. Instrum., 3, 219-228, 1977.

Michel, F. C., Solar-wind interaction with the field-free planets, Comments Astrophys. Space Phys., 3, 27-31, 1971a.

Michel, F. C., Solar-wind induced mass loss from magnetic field-free planets, Planet. Space Sci., 19, 1580-1583, 1971b.

Mihalov, J. D., H. R. Collard, J. H. Wolfe, and A. Frosolone, Solar wind activity in 1979 as observed by the Pioneer Venus orbiter (abstract), Eos Trans., AGU, 60, 931, 1979.

Pérez de Tejada, H., and M. Dryer, Viscous boundary layer for the Venusian ionopause, J. Geophys. Res., 81, 2023-2029, 1976.

Romanov, S. A., V. N. Smirnov, and O. L. Vaisberg, Interaction of the solar wind with Venus, Cosmic Res., 16, 603-611, 1979.

Russell, C. T., The interaction of the solar wind with Mars, Venus, and Mercury, in Solar System Plasma Physics, Vol. 2, Magnetospheres, edited by C. F. Kennel, L. J. Lanzerotti, and E. N. Parker, pp. 207-252, North-Holland, Amsterdam, 1979.

Russell, C. T., R. C. Elphic, and J. A. Slavin, The solar wind interaction with Venus, in Proceedings of Magnetospheric Boundary Layers Conference, pp. 231-239, European Space Agency, Alpbach, Austria, 1979a.

Russell, C. T., R. C. Elphic, and J. A. Slavin, Pioneer magnetometer observations of the Venus bow shock, Nature, 282, 815-816, 1979b.

Sanderson, J. J., and R. A. Uhrig, Jr., Extended Rankine-Hugoniot relations for collisionless shocks, J. Geophys. Res., 83, 1395-1400, 1978.

Scarf, F. L., W. W. L. Taylor, C. T. Russell, and R. C. Elphic, Pioneer-Venus plasma wave observations: The solar wind-Venus interaction, J. Geophys. Res., this issue.

Shefer, R. A., A. J. Lazarus, and H. S. Bridge, A reexamination of plasma measurements from the Mariner 5 Venus encounter, J. Geophys. Res., 84, 2109-2114, 1979.

Slavin, J. A., R. C. Elphic, C. T. Russell, J. H. Wolfe, and D. S. Intriligator, Position and shape of the Venus bow shock: Pioneer Venus orbiter observations, Geophys. Res. Lett., 6, 901-904, 1979a.

Slavin, J. A., R. C. Elphic, and C. T. Russell, A comparison of Pioneer Venus and Venera bow shock observations: Evidence for a solar cycle variation, Geophys. Res. Lett., 6. 905-908, 1979b.

Slavin, J. A., R. C. Elphic, C. T. Russell, F. L. Scarf, J. H. Wolfe, J. D. Mihalov, D. S. Intriligator, L. H. Brace, H. A. Taylor, Jr., and R. E. Daniell, Jr., The solar wind interaction with Venus: Pioneer Venus observations of bow shock location and structure, J. Geophys. Res., this issue.

Smirnov, V. N., O. L. Vaisberg, and D. S. Intriligator, An empirical model of the Venusian outer environment, 2. The shape and location of the bow shock, submitted to J. Geophys. Res., 1979.

Spenner, K.,W. C. Knudsen, K. L. Miller, K. Novak, C. T. Russell, and R. C. Elphic, Observation of the Venus mantle: The boundary region between solar wind and ionosphere, J. Geophys. Res., this issue.

Spreiter, J. R., A. L. Summers, and A. Y. Alksne, Hydromagnetic flow around the magnetosphere, Planet. Space Sci., 14, 223-253, 1966.

Spreiter, J. R., A. L. Summers, and A. W. Rizzi, Solar wind flow past nonmagnetic planets-Venus and Mars, Planet. Space Sci., 18, 1281-1299, 1970.

Spreiter, J. R., and A. W. Rizzi, Aligned magnetohydrodynamic solution for solar wind flow past the earth's magnetosphere, Acta Astronaut., 1, 15-35, 1974.

Spreiter, J. R., and S. S. Stahara, Theoretical properties of solar wind flow past Venus, J. Geophys. Res., this issue.

Stahara, S. S., D. Klenke, B. C. Trudinger, and J. R. Spreiter, Application of advanced computational procedures for modeling solar-wind interactions with Venus-theory and computer code, Report NEAR TR 202, Nielsen Engineering and Research, Inc., Mountain View, Calif., 1979.

Taylor, H. A., Jr., H. C. Brinton, S. J. Bauer, R. E. Hartle, T. M. Donahue, P. A. Cloutier, F. C. Michel, R. E. Daniell, Jr., and B. H. Blackwell, Ionosphere of Venus: First observations of the dayside ion composition near dawn and dusk, Science, 203, 752-754, 1979a.

Taylor, H. A., Jr., H. C. Brinton, S. J. bauer, R. E. Hartle, P. A. Cloutier, F. C. Michel, R. E. Daniell, Jr., T. M. Donahue, and R. C. Maehl, Ionosphere of Venus: First observations of the effects of dynamics on the dayside ion composition, Science, 203, 755-757, 1979b.

Taylor, H. A., Jr., H. C. Brinton, S. J. Bauer, R. E. Hartle, P. A. Cloutier, R. E. Daniell, Jr., and T. M. Donahue, Ionosphere of Venus: First observations of day-night variations of the ion composition, Science, 205, 96-99, 1979c.

Taylor, H. A., Jr., H. C. Brinton, S. J. Bauer, R. E. Hartle, P. A. Cloutier, and R. E. Daniell, Jr., Global observations of the composition and dynamics of the ionosphere of Venus: Implications for the solar wind interaction, J. Geophys. Res., this issue.

Tidman, D. A., and N. A. Krall, Shock Waves in Collisionless Plasmas, Interscience, New York, 1971.

Vaisberg, O. L., S. A. Romanov, V. N. Smirnov, I. P. Karpinsky, B. I. Khazanov, B. V. Polenov, A. V. Bogdanov, and N. M. Antonov, Ion flux parameters in the solar wind-Venus interaction region according to Venera-9 and Venera-10 data, in Physics of Solar Planetary Environments, vol. 2, edited by D. J. Williams, pp. 904-917, American Geophysical Union, Washington, D. C., 1976.

Verigin, M. I., K. I. Gringauz, T. Gombosi, T. K. Breus, V. V. Bezrukikh, A. P. Remizov, and G. I. Volkov, Plasma near Venus from the Venera 9 and 10 wide-angle analyzer data, J. Geophys. Res., 83, 3721-3728, 1978.

Wallis, M. K., Weakly-shocked flows of the solar wind plasma through atmospheres of comets and planets, Planet. Space Sci., 21, 1647-1660, 1973.

Wolfe, J. H., and D. D. McKibbin, Pioneer 6 observations of a steady-state magnetosheath, Planet. Space Sci., 16, 953-969, 1968.

Wolfe, J. H., D. S. Intriligator, J. D. Mihalov, H. Collard, D. McKibbin, R. Whitten, and A. Barnes, Initial observations of the Pioneer Venus orbiter solar wind plasma experiment, Science, 203, 750-752, 1979.

(Received December 20, 1979;
revised May 27, 1980;
accepted May 28, 1980.)